

Universal geometric transformation method PGT for aircraft design

Alexander Nikolsky, anikolskiii@gmail.com, Central Aerohydrodynamic Institute named after Professor N. E. Zhukovsky, Russia

The original technique for CAD/ CAE applications of generating aerodynamic shapes is developed. The universal geometric 'parent function/generating functions' transformation method, PGT, is proposed which creates the compact design space covering the entire class of wireframe contours for the design of basic aircraft elements

The wireframe concept is commonly used for surface generation of basic elements of aircraft, such as wing, blade, control surfaces and fuselage. From the one hand it is important to parameterize a wireframe with a reasonable accuracy for CAD applications; from another hand it is important to establish a minimal parameters amount for reaching the accuracy sufficient for CAE design applications. The known techniques of parameterization [1- 7] are based on limited class of functions and not suitable for an arbitrary geometry representation. So it is important to find a universal mathematical formulation to cover the entire set of possible wireframe shapes. Further the basic principles of a new approach are outlined.

1. WIREFRAME OF WING/BLADE TYPE

1.1 AIRFOIL SPLINE

First, consider the wireframe consisting of wing/blade cross sections and its basic element, an airfoil. For definiteness consider the upper airfoil surface, represented by tabular function $y_i(x_i), i = 1, \dots, N$ and perform a coordinate transformation: $\xi = \sqrt{x}$, which allows removing singularity at the rounded nose

at $x = 0$. If r_u is the radius of the upper nose curvature, then $\frac{dy}{d\xi}(0) = \sqrt{2r_u}$. Now in the auxiliary $\xi - y$ plane the tabular function can be interpolated by a conventional cubic spline called airfoil spline $S_N^{(a)}$. Its first design application is published in [8]:

$$S_N^{(a)}(\xi) = \sum_{k=0}^3 a_i (\xi - \xi_i)^k, i = 1, \dots, N$$

When the number of points m is taken less than N , this spline approximates a function $y(x)$ with the certain accuracy, which is necessary to establish. Further, the sequence of m breakpoints $\xi_i, i = 1, \dots, m$ along an airfoil chord in plane $\xi - y$ is called a division and denoted D_m . There were explored some array of airfoils (more than 10) and the different variants of division (in number of points and their location along the chord) with concentration points at the edges of the airfoils. The numerical experiments consisted in approximating an actual geometry by splines $S_m^{(a)}$, interpolating on basic division D_N and calculating the flow about airfoils obtained. Full potential (FPE) simulations were considered as a

good test because of one-to-one correspondence between the pressure coefficients $C_p(x)$ and airfoil geometry. Eventually established were three specific divisions: D_{29} , D_{15} and D_{10} . The points of a coarser division are included in the finer division (see Figure 1.). Further analysis is mainly based on the calculated data obtained for the familiar helicopter VR12 airfoil, tabulated in 41 upper and lower points [9].

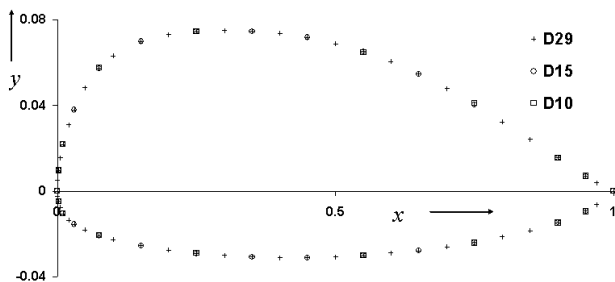


Figure.1: Breakpoints locations along airfoil chord.

The accuracy of the geometry approximation is estimated in Figure 2, where $\delta_s = S^{(a)}(x) - y_U(x)$ is the ordinate deviations of approximated (D_{29}) airfoil from actual airfoil (D_{41}).

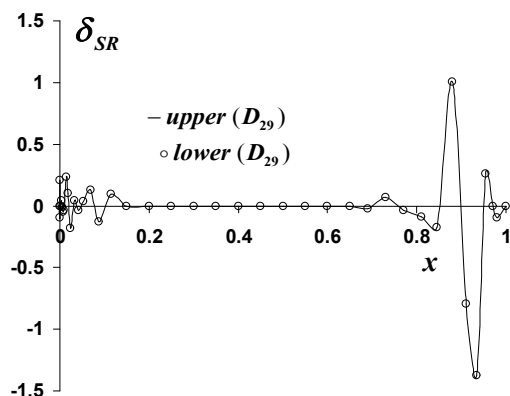


Figure 2: Estimation of geometrical accuracy of the basic airfoil spline approximation

The following relation is satisfied along most of the chord: $\delta_s \ll \delta_s^{wt}$. Here

$\delta_s^{wt} = 3 \div 7 \cdot 10^{-4}$ is a typical wind tunnel model tolerance. Some amplitude rising in the tail part is explained by the smoothing effect (desirable) due to reducing the number of points. Further on the charts the designation $\delta_{SR} = \delta_s \cdot 10^4$ is used.

This fact is illustrated in Figure 3, where the curvature of the upper surfaces of the actual and approximated airfoils are depicted.

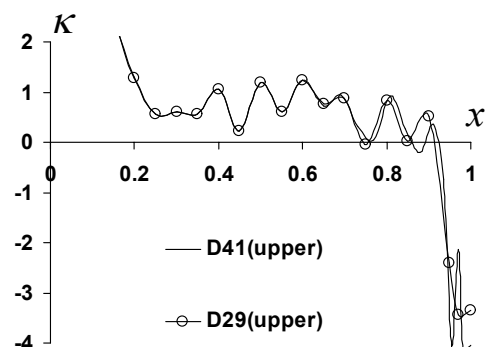


Figure 3: Curvature of the upper surfaces of the actual and approximated airfoils

The corresponding pressure distributions coefficients C_p at $M = 0.8$, $C_L = 0$ are depicted in Figure 4. Here M - the Mach number, C_L - lift coefficient.

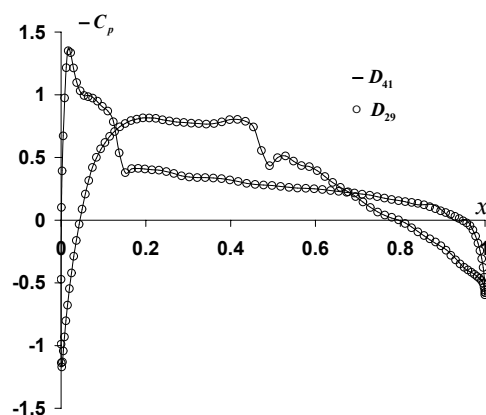


Figure 4 : Estimation of aerodynamic accuracy of basic airfoil spline approximation

One can see a perfect match of the pressure diagrams. Similar practically a global match is also observed at other flow conditions, and for the whole array of

airfoils examined. Thus, spline $S_{29}^{(a)}$, based on a division D_{29} with necessary and sufficient accuracy approximates, in general, arbitrary airfoil geometry. Further, for brevity, this spline is called a basic airfoil spline $S_B^{(a)}$. This spline may be considered as a suitable and accurate analytical representation of wireframe elements of wing/blade type for CAD/CAE applications.

For smoothing a curvature instead of the spline $S_B^{(a)}$ one can use a smoothing basic airfoil spline $S_{Bsm}^{(a)}$. Recall that all the splines are generating in the $\xi - y$ plane, where the derivative $\frac{dy}{d\xi}(0)$ is finite. The smoothing parameters were chosen in a way that reduces the deviation in the range $|\delta_{SR}| < 1$, as depicted in Figure 5.

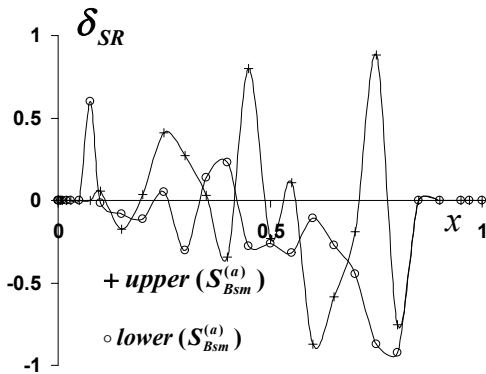


Figure 5: Estimation of geometrical accuracy of the basic ordinary and smoothing airfoil splines approximation

Curvature of the upper airfoil surfaces approximated by base ($S_B^{(a)}$) and smoothed base ($S_{Bsm}^{(a)}$) splines are depicted in Figure 6. This smoothing does not degrade the agreement observed in Figure 4, so spline $S_{Bsm}^{(a)}$ may be considered as an alternative form of basic airfoil spline.

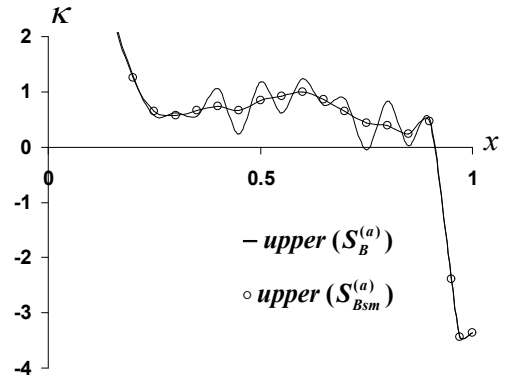


Figure 6: Curvature of the upper surface curve approximated by the two types of basic spline

1.2 AERODYNAMIC AIRFOIL SPLINE

For the purposes of the aircraft design the number of design variables must be minimized, but still possible to get airfoil performances with sufficient accuracy. The one of the best way to check the aerodynamic accuracy is solving an inverse problem. The target pressure distributions were predicted by FPE simulation. The inverse problems were solved by minimizing of the functional J , equivalent to the standard deviation of the pressure distribution from the target:

$$J = \sqrt{\sum_{i=1}^M \Delta(C_{pi} - C_{pTi})^2 / N}. \text{ Here } C_{pT} - \text{ the}$$

target pressure distribution (D_{29}). A set of $y_{ui}(\xi_i)$ and $y_{li}(\xi_i)$, $i = 1, \dots, m$ were used as the design variables Since the locations of the leading and trailing edges of the airfoil are fixed, the design variables number becomes $m_{DV} = 2(m-2)$. It was found that the effectiveness of the optimization procedure can be improved by alternating using of two subspaces of design variables $y_{ui}(\xi_i)$ and $y_{li}(\xi_i)$, wherein $m_{DV} = m$. The second factor in accelerating the procedure was to use the coarse division solution as an initial approximation for calculating the fine division solution.

Based on comparison of the inverse problems solutions for array of airfoils and divisions there were established minimum final division D_{10} and the division D_{15} having an approximating accuracy of calculated pressure distribution near to the basic division, D_{29} . Full comparative analysis was carried out for three specific helicopter airfoils flow conditions: $M = 0.4$, $C_L = 1.5$ (near $C_{L_{max}}$); $M = 0.6$, $C_L = 0.6$ (near $(C_L / C_D)_{max}$); $M = 0.8$, $C_L = 0$ (near M_{DD}). Here M_{DD} - the drag divergence Mach number, $C_{L_{max}}$ - maximum lift coefficient, C_D - drag coefficient.

Data are presented for airfoils based on approximating splines (divisions D_{10} , D_{15} , basic D_{29}), and the airfoil obtained from the inverse problem solution (division D_{10}), designated in figures as $D_{10} (inv)$. The pressure distributions curves for the divisions D_{15} and $D_{15} (inv)$ in all regimes are practically identical with target pressure distribution (so graphs are omitted). Pressure distributions curves for division D_{10} at subsonic regimes are also close to the target distributions.

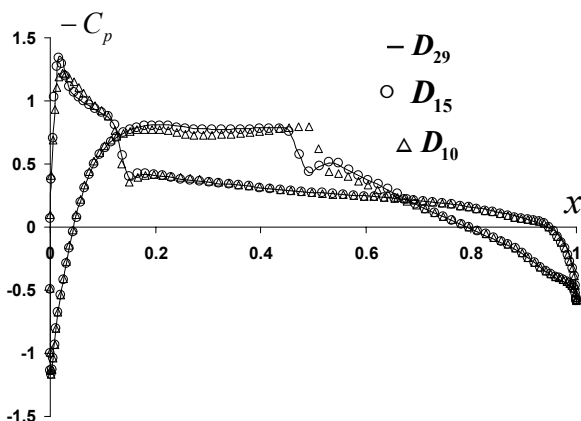


Figure 7 The pressure distribution over original (D_{29}) and approximated airfoils, $M = 0.8$, $C_L = 0$, FPE predictions

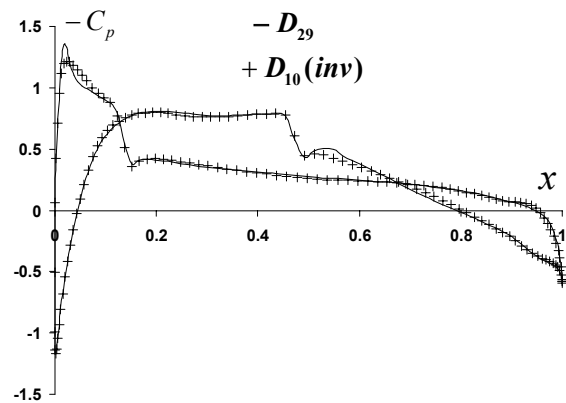


Figure 8: The pressure distribution over original (D_{29}) and optimized airfoils, $M = 0.8$, $C_L = 0$, FPE predictions

However, at transonic regime, Figures 7,8 show that the pressure distribution of the inverse problem solution, $D_{10} (inv)$, is in more better agreement with the target pressure distribution than that one for approximated airfoil, D_{10} .

In order to evaluate the quantitative aerodynamic accuracy, the performances of the studied airfoils were predicted by CFD RANS calculations. Figures 9, 10 illustrate an excellent agreement of dependences $C_L(\alpha)$ and $C_L(C_D)$ with target ones (D_{29}) at subsonic regimes.

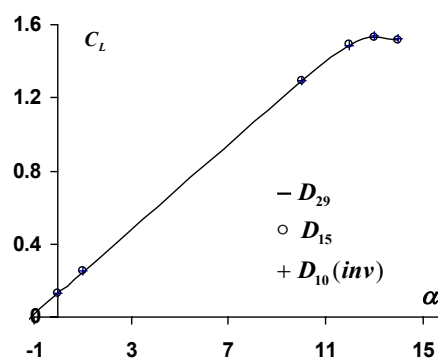


Figure 9: Lift curve vs of AoA, $M = 0.4$

The same tendency is observed at transonic regimes (see Figures 11, 12), only slight difference in dependencies $C_{m0}(M_\infty)$ and $C_{D0}(M_\infty)$ is observed and the M_{DD} values are almost coincide.

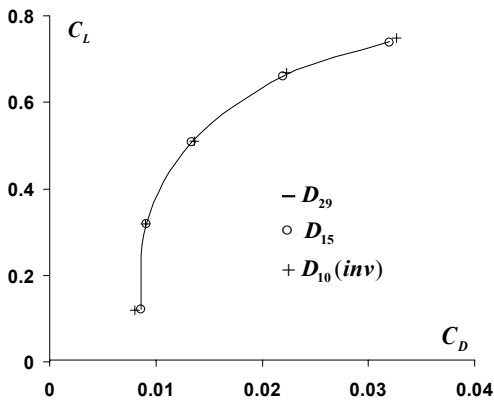


Figure 10: Drag coefficient vs lift coefficient, $M=0.6$

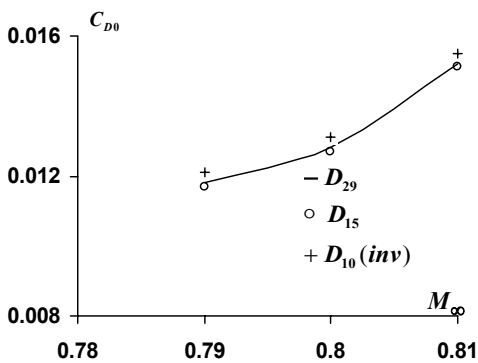


Figure 11: Drag coefficient at zero lift vs Mach number

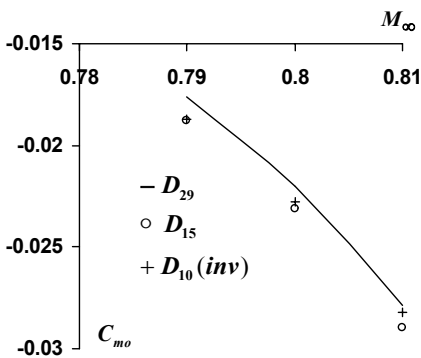


Figure 12: Pitching moment coefficient at zero lift vs Mach number

The similar results (qualitative and quantitative) were obtained for the array of airfoils considered. Thus, it is important that the geometry of the airfoil with accuracy sufficient for the aerodynamic design can be parameterized by splines

$S^{(a)}$ constructed from about 10 points, and the aerodynamic performances of the multiregime airfoils can be optimized using about 20 design variables, involving in the optimization process alternately two groups of 10 variables. This spline is called aerodynamic airfoil spline and denote $S_A^{(a)}$.

If necessary, the optimization process may consist of an additional qualifying phase. At this stage the number of points may be increased. It does not complicate a procedure because of computer code stays the same. Only one string has to be read for changing the division.

It should be recalled that the claimed results are confirmed on a limited array of airfoils. However, they seem to be valid for any wing/blade wireframe made up of smooth curves.

1.3 WIREFRAME OF FUSELAGE TYPE

The cross sections curve of fuselage type body has a two rounded edges.

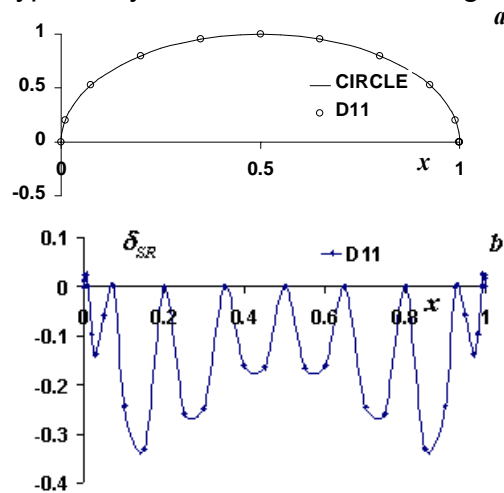


Figure 13: a- points locations; b- Estimation of geometrical accuracy of the body spline approximation

So to eliminate an additional singularity one can use another coordinate transformation $\xi = \arccos(1 - 2\sqrt{x}) \pi$. Repeating above analyses one gets a body spline representation $S^{(b)}$ in a new ξ - y plane. For example Figures 13 b

confirms the good accuracy of circle approximation by spline $S^{(b)}$ based on division D_{11} . The points distribution is depicted in figure 13 a.

Finally, one can notice that the splines $S^{(a)}$ and $S^{(b)}$ can be used in generating a complex 3-d wireframe geometries in CAD systems and in fast regenerating of the computational meshes. These splines can as well be used for forming a universal (in number and location of points along the chord) of the geometric aircraft database. Moreover, any geometrical wireframe parameters can be determined analytically.

2 UNIVERSAL PGT METHOD

2.1 PARENT AND GENERATING FUNCTIONS

However for CAE optimization using points $y_i, i=1, \dots, m$ as the design variables is not always effective due to additional shape control and overlapping the ranges of their changing. So an alternative original method PGT [10] was developed.

Let's upper and lower surface curves are defined as $y_u(\xi) = y_{u\max} f_u(\xi)$ and $y_l(\xi) = y_{l\min} f_l(\xi)$, where $y_{u\max}$ and $y_{l\min}$ are maximums of functions. The 'parent' function one defines as follows: $f_p = 4\xi(1-\xi)$. Notice that the sets of values of functions f_p, f_u, f_l are arranged in the same manner as in Figure 14. It allows using the simple relations to define functions generating an

arbitrary airfoil family: $\xi_u = \frac{(1 \pm \sqrt{1-f_u})^2}{2}$,

$\xi_l = \frac{(1 \pm \sqrt{1-f_l})^2}{2}$. These generating

functions for VR12 airfoil are depicted in Figure 15.

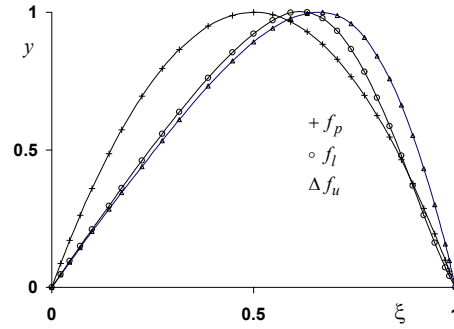


Figure 14 Scaled shape functions and parent function

Two curves $\xi_u(\xi)$ and $\xi_l(\xi)$ look as chromosomes and sequences ξ_{ui} and ξ_{li} as chains of genes defining geometric airfoil family genotype. By adding two additional genes $y_{u\max}$ and $y_{l\min}$ one obtains a unique instance of the airfoil family. When f_u or f_l is not monotonic after its maximum it is replaced by f_l based on airfoil thickness distribution which is usually monotonic.

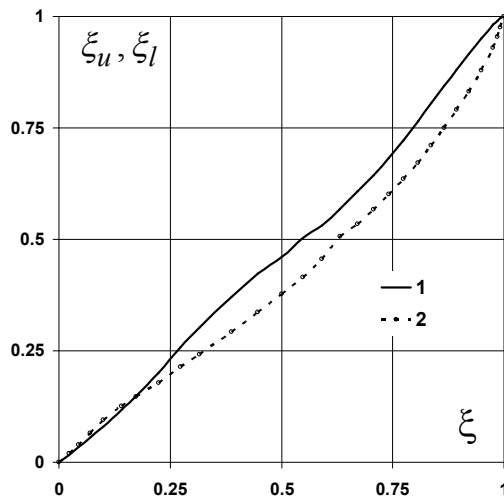


Figure 15: Generating functions for VR-12 airfoil. 1- $\xi_u(\xi)$, 2- $\xi_l(\xi)$

It is necessary to note that functions $\xi_u(\xi)$, $\xi_l(\xi)$ and $\xi_i(\xi)$ are monotonically increasing from 0 to 1 and belong to limited class of functions but cover the entire class of possible airfoil shapes. For

interpolating in $\xi_u - \xi$ plane an ordinary cubic spline, called **ksi-spline**, is used.

The compact design space for blade/wing design has a simple interpretation as a closed region on $\xi_u - \xi$ plane, as shown in Figure 16 for an array of airfoils. Using low fidelity solver predictions the design space may be simply reduced for more economical high fidelity solver calculations. Besides the number of design variables may be changed in the design process without additional coding.

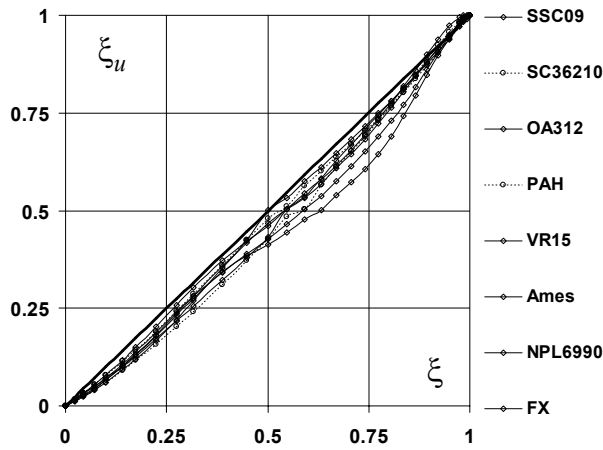


Figure 16: Design variables space

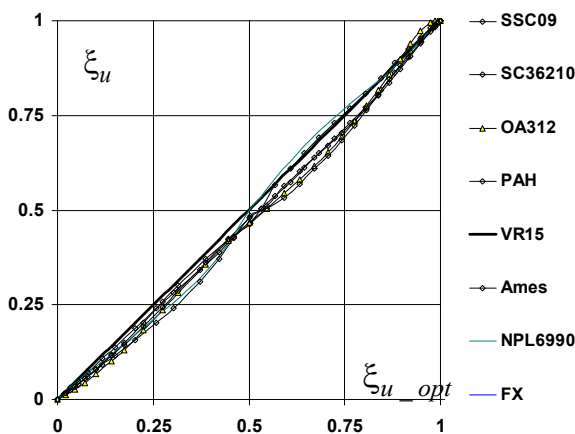


Figure 17: Alternative design variables space

Thus PGT method, based on design variables ξ_{ui}, ξ_{li} or ξ_{ti} , $i=2, \dots, 9$, using splines $S_A^{(a)}$ with total about 18 design variables seems to be a perspective optimization technique.

It is clear that instead of $\xi_u - \xi$ design plane one may use $\xi_u - \xi_{u_opt}$ design plane, where ξ_{u_opt} is a generating function for a solution optimal at that moment. The dependency $\xi_u(\xi_{u_opt})$ demonstrates how the next airfoil geometry constructs from a previous geometry.

It is an additional provement of universality of PGT method.

Another interesting design plane is $\xi_u - \xi_t$ plane. For many airfoils the dependency $\xi_u(\xi_t)$ is near to a linear dependency (see Figure 18).

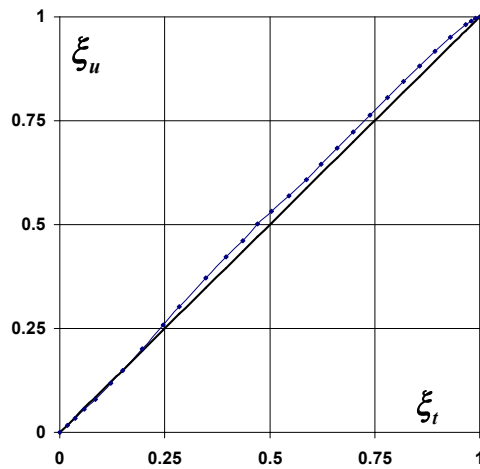


Figure 18: VR-12 airfoil design variables space

Note, that for airfoil with finite trailing edge thickness the parent function has a more complicated form:

$$f_p = 4a_p \xi (1 - a_p \xi), \text{ where}$$

$$a_p = (\sqrt{1 - \delta_{te} / y_{\max}} + 1) / 2.$$

2.2 COMPARISON OF PGT AND CST PARAMETERIZATIONS

Recently, in many studies, the CST method [6] of airfoil parameterization (Class Function/ Shape function Transformation) has become very popular. In this method, the airfoil curves are represented in the following form: $y = \sqrt{x}(1-x)s(x)$. The function $c(x) = \sqrt{x}(1-x)$ is called the class function, the function $s(x)$ is called the shape function, and its form is declared as: $s(x) = \sum_{i=0}^{\infty} a_i x^i$. Further, following this suggestion, the function $s(x)$ has a finite derivative at $x=0$: $s'(0) = a_1$. In fact, these arguments are valid only for a limited subclass of possible curves. Obviously, in the neighborhood of point $x=0$, an arbitrary curve, having finite curvature of the leading edge radius, R , can be represented in the form: $y = \sqrt{2Rx} + O(x^\alpha)$, where $\alpha \geq 1$. This implies the general asymptotic expansion for the shape function: $s(x) = \sqrt{2R} + O(x^{\alpha-1/2})$ and asymptotic expansion for its derivative: $s'(x) \sim O(x^{\alpha-3/2})$.

Therefore, the declaration of the finiteness of the derivative of the shape function at $x=0$, as well as the CST method itself, is valid only for $\alpha \geq 3/2$. Such a restriction, of course, narrows the class of airfoil shapes, the parameterization of which is possible with the CST method. For example, a classic polynomial function has a form:

$$y(x) = b_0 \sqrt{x} + \sum_{i=0}^{\infty} b_i x^i$$

It generates a shape function having an infinite derivative at $x=0$, if $b_1 \neq 0$. Thus, in

general the introduction of a class function does not allow eliminating the singularity of the derivative of the shape function.

The PGT technique and the concept of an airfoil spline make it possible to formulate a really "fundamental" parameterization method, covering a general class of airfoil geometries without any restrictions.

In PGT technique the parent function is used instead of class function. Generating functions always have no singularity ($\frac{d\xi_u}{d\xi}(0) = \sqrt{r_c/8}$) and play the role of shape function. For airfoil spline parameterization the role prescribed to the class function performs an elementary coordinate transformation, $\xi = \sqrt{x}$. The role of the shape function performs the function $y(\xi)$ always having a finite derivative in the auxiliary $\xi-y$ plane.

Taking into account the finiteness of the derivative of the functions $y(\xi)$, $\xi_u(\xi)$ we have a sufficient reason to approximate them by the Bernstein polynomial of order

$$n: \text{BPO}_n(x) = \sum_{r=0}^n K_{r,n} (1-x)^{n-r} x^r$$

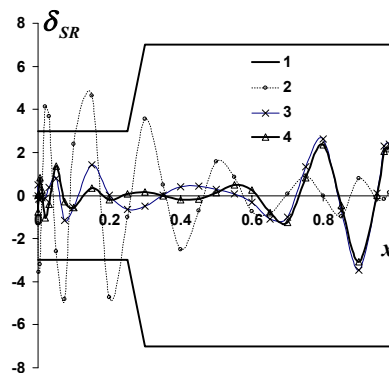


Figure 18: Approximations accuracy of SSC-A09 airfoil upper surface: 1- WTT; 2- CST(BPO15); 3- $y(\xi)$ (BPO11), PGT(BPO11)

In the case of $y(\xi)$ approximation one obtains the following analytical approximation of arbitrary tabular function $y(x)$:

$$y(x) = \sum_{r=0}^n a_r (1 - \sqrt{x})^{n-r} x^{r/2}. \quad \text{This original}$$

representation has no analog in literature. Figure 18 shows the typical wind tunnel model coordinates tolerances WTT, and the differences between the actual upper surface coordinates of the Sikorsky SSC-A09 airfoil and coordinates of the airfoil approximated by the CST method using the 15th degree Bernstein polynomial (BPO15) and coordinates of this airfoil, approximated in the $\xi - y$ plane and $\xi_u - \xi$ plane by the Bernstein polynomial of the 11th degree (BPO11). The present methods provide a good approximation because of no restrictions imposed. Minor differences in the tail region are due to the smoothing effect when the fast changing curvature of tabular function takes place. The unsatisfactory CST approximation in the vicinity of the leading edge is due to an incorrect declaration (in this case) of the finiteness of the derivative of the shape function at $x = 0$.

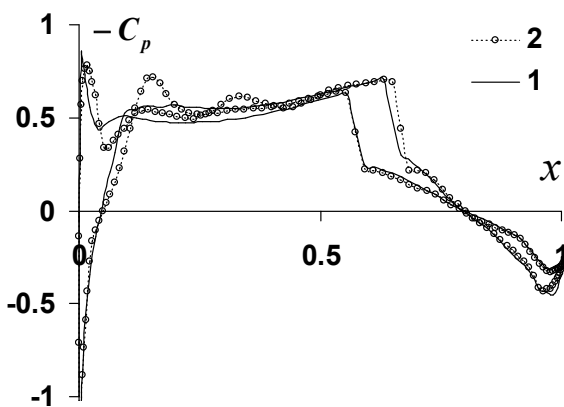


Figure 19: Pressure distributions: 1- actual airfoil; 2- CST(BPO15)

Figure 19 confirms that not always the CST approximation method leads to satisfactory results. The similar conclusion is valid for OA family airfoils.

In contrast, the approximation by the presented techniques reproduces the actual distribution of the pressure coefficient with the good accuracy. The data presented clearly demonstrate that it is the $S^{(a)}$ and PGT technique that allows to obtain a fundamental parametric representation of the airfoil geometry.

2.3 DETAILS OF PGT METHOD

Notice, the use of Bernstein polynomial coefficients as design variables is limited by the fact that it is problematic to establish the range of their variation needed to localize the space of design variables when searching for the global optimum of the objective function. Therefore, apparently, the area of their application is limited to the search for a local optimum in the neighborhood of a known geometry. So the generating the geometry in PGT technique uses the following steps:

- 1 Generating the design space in $\xi_u - \xi$ plane (see Figure 16);
- 2 Choosing the design variables division D_m , and giving $\xi_{ui}(\xi_i)$, $i=1, \dots, m$;
- 3 Ordinary spline interpolating the function ξ_u known at m design points to fit the basic distribution, ξ_{Bi} , $i=1, \dots, M$, needed for detailed geometry description and flow simulations;

Sometimes to improve the convergence at the beginning of the design process interpolated functions $\xi_u(\xi)$ needs smoothing to avoid not aerodynamical shape, so it may be the additional step 4:

- 4 Approximating (simultaneously smoothing) the function $\xi_u(\xi)$ by Bernstein polynomial or by smoothing cubic spline (see Figure 20).

Recall that entire airfoil geometry is generated by two of the three functions

$\xi_u(\xi)$, $\xi_l(\xi)$, $\xi_t(\xi)$ and two of three parameters $y_{u\max}$, $y_{l\min}$, $y_{t\min}$ respectively.

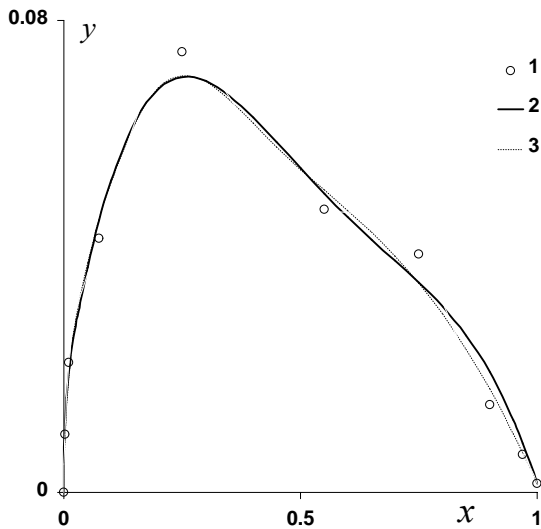


Figure 19: Coordinate smoothing: 1- design curve; 2- $\xi_u(\xi)$ (BPO6); 3- smoothing spline

CONCLUSIONS

The universal wireframe geometry representation is illustrated on the example of 2D wireframe elements of airfoil and “body” types. When wireframe consists of not plane elements the 3d curve maybe decomposed on two plane curves.

This technique allows providing one-to-one reproducing an arbitrary wing/blade/body tabular wireframe curve with generating & parent functions. Two ways of approximation and parameterization for aircraft design are described. The first uses a concept of airfoil/body splines, and the second- a concept of **ksi**-splines.

The universality of PGT geometry is demonstrated by the possibility of building one airfoil geometry from another arbitrary geometry.

Copyright Statement

The author confirms that he and its organization hold copyright on all of the original material included in this paper. The author confirms that he gives permission for the publication and distribution of this paper as part of the ERF2018 proceedings or as individual offprints from the proceedings and for inclusion in a freely accessible web-based repository.

References

- [1] Sobieczky, H.. Parametric Airfoils and Wings, “Notes on Numerical Fluid Mechanics ,Vieweg Verlag, Vol. 68, pp.71-88, 1998.
- [2] Robinson, GM, and Keane. AJ, Concise Orthogonal Representation of Supercritical Airfoils. Journal of Aircraft, Vol. 38, No. 3, pp. 580-583, 2001.
- [3] Padula, S., and Li, W., Options for Robust Airfoil Optimization Under Uncertainty. 9th AIAA Multidisciplinary Analysis and Optimization Symposium, paper No. 2002-5602, pp.1-7, 2002.
- [4] Song, W., and Keane, AJ, A Study of Shape Parameterisation Airfoil Optimisation . AIAA-2004-4482, 10th AIAA / ISSMO Multidisciplinary Analysis and Optimization Conference, pp.1-8, 2004.
- [5] Samareh, JA. Aerodynamic Shape Optimization Based on Free-Form Deformation. AIAA 2004-4630, pp.1-6, 2004.
- [6] B. M. Kulfan. Recent extensions and applications of the ‘CST’ universal parametric geometry representation method. The Aeronautical Journal, 2010, vol. 114, no. 1153, pp. 157-176.
- [7] Nikolsky A.A. Some aspects of helicopter airfoil design // Twenty first european rotorcraft forum. -1995. –V. 2. –N 17. -8 p.

[8] Nikolsky A.A. Optimization of the leading edges of helicopter airfoils. Tsagi Science Journal, 2008, vol. 39, no. 4, pp. 5-8, in Russian.

[9] Dadone LU Advanced airfoils for helicopters rotor application, US Patent No 4,341,795, 1982.

[10] Nikolsky A.A. About a geometric genotype of shapes of airfoils. Tsagi Science Journal, 2014, vol. 45, no.5, pp. 417-429